Gigacycle fatigue initiation mechanism in Armco iron

Chen Wang, D. Wagner, Q. Y. Wang, C. Bathias

Gigacycle fatigue initiation mechanism in Armco iron

C. Wang [a,b], D. Wagner [a], Q.Y. Wang [b], C. Bathias [a,*]

[a] Université Paris Ouest Nanterre La Défense, LEME, 50 Rue de Sèvres, 92410 Ville d'Avray, France
[b] Department of Civil Engineering and Mechanics, Sichuan University, Chengdu 610065, China

Keywords:
Gigacycle fatigue
Persistent slip bands
Grain boundary
Crack initiation
Iron

A B S T R A C T

Microstructure irreversibility plays a major role in the gigacycle fatigue crack initiation. Surface Persistent Slip Bands (PSB) formation on Copper and its alloy was well studied by Mughrabi et al. as typical fatigue crack nucleation in the very high cycle fatigue regime. In the present paper, Armco iron sheet specimens (1 mm thickness) were tested under ultrasonic frequency fatigue loading in tension–compression ($R = -1$). The test on the thin sheets has required a new design of specimen and new attachment of specimen. After gigacycle fatigue testing, the surface appearance was observed by optical and Scanning Electron Microscope (SEM). Below about 88 MPa stress, there is no PSBs even after fatigue cycle up to 5×10^9. With a sufficient stress (above 88 MPa), PSBs in the ferrite grain was observed by optic microscope after 10^8 cycles loading. Investigation with the SEM shows that the PSB can appear in the body-centered cubic crystal in the gigacycle fatigue regime. Because of the grain boundary, however, the local PSB did not continually progress to the grain beside even after 10^9 cycles when the stress remained at the low level.

1. Introduction

Approaching 10^9 cycles the plastic deformation in plane stress conditions is vanishing; the macroscopic behavior of the metal is elastic except around flaws, metallurgical defects or inclusions. In very high cycle fatigue, the plane stress conditions according to the Von Mises criteria related to the surface plastic deformation are in competition with the stress concentration around flaws. The initiation may be located in an internal zone. When the crack initiation site is in the interior, this leads to the formation of one fish eye on the fracture surface, typical of gigacycle fatigue [1–4]. In this case, the cyclic plastic deformation related to the stress concentration around a defect: inclusion, porosity, super grain. Since the probability of occurrence of a flaw is greater within internal volume than at a surface, the typical initiation in gigacycle fatigue will be most often in the bulk in the metal. This is the case for many industrial alloys. However, for a basic point of view, it is of interest to understand the initiation of a fatigue crack in the gigacycle regime in pure alloys or metals without internal defect or with very small defect.

If there is no critical flaw in the metal, the plane stress effect is supposed to be enough efficient to nucleate plastic deformation at the surface. In order to study this phenomenon a flat specimen, easy for microscopic observation, was designed to be tested at 20 kHz up to 10^9 cycles.

The first fatigue investigation carries out on iron at ultrasonic frequency (17 kHz) by Wood and Mason after this technology successful used on f.c.c. metal [5]. By loading amplitude much less than the safe limit of the low frequency fatigue (1700 cpm), isolated slip lines appear in occasional grains which similar slip line concentrations of deformation characterized on the f.c.c. metal. They noticed a difference about observation on specimen surface between low frequency and high frequency tested. With several times higher amplitude in low frequency test, concentration of deformation in the grain boundaries instead of localized slip line in high frequency lower amplitude.

Puskar compared formation of crack and slip band in iron at various temperatures controlled by flow of nitrogen with notch specimen at ultrasonic frequency (23 kHz) [6]. He pointed out that the surface layer and grain boundary play significant role in the process of crack propagation at high frequency loading at different temperature. The fatigue crack initiates in surface layer from slightly dense slip bands, subgrain boundaries, grain boundaries or in regions without slip bands. Number of grain that shows these slip lines is a parabolic function of both amplitude and temperature. He also compared fatigue of iron tested under ultrasonic frequency and low frequency and concluded that fatigue crack initiation and propagation at ultrasonic frequency are similar to those at lower frequency loading.

Studies tested at different conditions of loading given references for investigating fatigue features at ultrasonic frequency on iron. Dislocation arrangement in iron after fatigue bending test at low frequency investigates by Mcgrath and Bratina [7]. They find

* Corresponding author. Tel.: +33 1 4027 23 22.
E-mail address: claude@bathias.com (C. Bathias).

that the average dislocation density for a particular stress amplitude reaches a constant value after showing a rapid increase in the early portion of the fatigue life. When Wood et al. [8] compare the fatigue mechanisms in bcc iron and fcc metals at low frequency in alternating torsion, they noted that at amplitudes above the SN knee, slip markings appeared on a specimen after a few cycles, at amplitude below the knee they appeared after a million or so cycles. That is the first second in the ultrasonic fatigue test. Wei and Baker find well developed arrays of dislocation loops in iron specimen after only 10 cycles in push–pull fatigue [9].

Klesnil and Lukas study the dislocation arrangement in the subsurface layer of iron grain by remove different thin layer in the surface [10]. The density of slip lines decreased as deeper in subsurface. The first microcrack appears on the boundaries of zone with a high dislocation density.

Many features of iron at low cycle fatigue descript by Mughrabi in the view of mono- and polycrystals, strain rate, PSB formation, carbon composition, temperature, asymmetry of slip and shape change [11–16]. However, fatigue deformation features of iron at very high cycle fatigue regime are limited. PSBs formation at subsurface and at initiation area was not well discussed on literature. Current work intends to investigating the fatigue initiation and localized irreversibility of body centered cubic (b.c.c.) metals Armco iron (α-Fe) at very high cycle fatigue regime.

2. Experimental detail

Investigations carried out on Armco iron that knows as typical b.c.c. metal. The chemical compositions indicate on Table 1 below. Metallographic on Fig. 1 shows a ferrite microstructure with grain size 10–40 μm. It has single phase with the inclusion size less than 1.5 μm. No specifically orientation was observed by EBSD graph. UTS is 300 MPa. Yield stress is 240 MPa.

To achieve the very high number of cycles as much as 10^9, piezoelectric ultrasonic fatigue system has the advantage of time saving and lowers cost. For the reason of surface observation condition, a new design of 1 mm thin specimen as shown in Fig. 2 was used to carry out fatigue testing. Specimen, special attachment and piezoelectric fatigue machine constituted the resonance system working at 20 kHz. Ultrasonic fatigue testing under cycle loading in tension–compression, $R = -1$. Special attachment and device were used to constrain transverse displacement and to avoid buckling when specimen working in tension–compression fatigue test, before testing, the thin flat specimen surface was prepared by different polishing and etching solution. Experiments were carried out at a temperature range 290–380 K.

3. Results and discussion

3.1. PSBs appearance

Mughrabi advised to distinguish the metal as Type I materials like copper or nickel face centered cubic (f.c.c) metals and Type II materials like high strength steel which usually contain heterogeneities [4]. Microstructural processes of fatigue crack initiation are different in these two types of metal. Very high cycle fatigue crack of Type I material always related to the formation of persistent slip bands on the surface [17–21]. On contrary, fractographic of Type II materials has "fisheye" as typical character after very high cycle

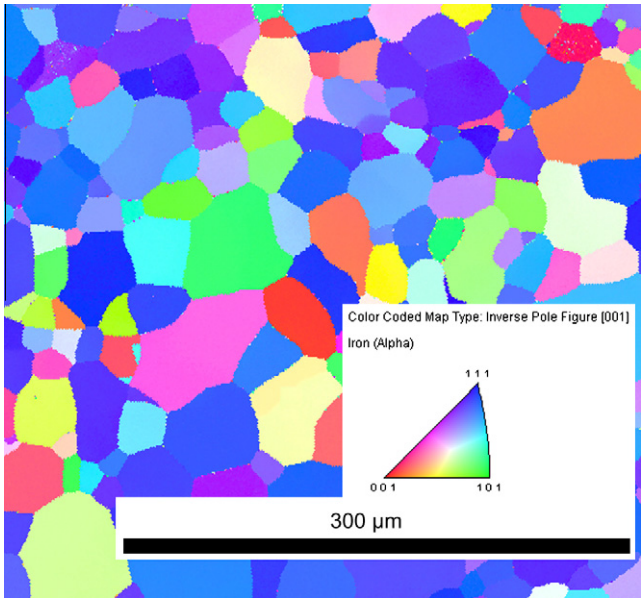

Fig. 1. metallographic orientation.

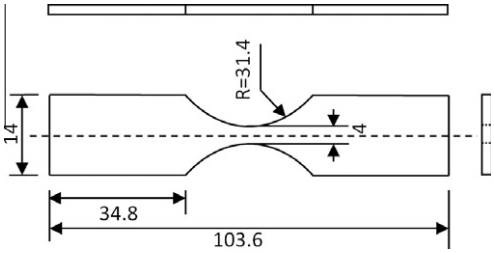

Fig. 2. Sketch of flat specimen (unit: mm).

fatigue testing [1–3]. However, α-Fe as basic industrial material was counted as neither Type I nor Type II materials.

Comparing the observations that performed on the surface of specimen before and after 10^8 cycles loading, arrows in Fig. 3 mark several PSBs appeared in the certain grain. PSBs inside of different grain have different orientation.

After 10^8 cycles with stress amplitude $\sigma_a = 111$ MPa, Fig. 4a shows PSBs occured almost saturated in one grain, where the neighbor grains have null appearance on the surface. In order to investigate the propagation of PSBs, micrograph 4b was taken after 2×10^9 cycles. The results suggest that those PSBs did not progress from 10^8 cycle to 2×10^9 cycles at stress remains 111 MPa. They are staying inside the grain except very slightly increase the width of PSBs.

3.2. PSBs at subsurface

In order to avoid effect from mechanical polishing and HNO_3 etching solution, specimen in Fig. 5a was electroliticaly polished but without etching. Micrograph taken after 10^8 cycle at $\sigma_a = 120$ MPa shows two distinguished PSBs appeared at surface of specimen with a form more straightly. It should be due to that

Table 1
Chemical compositions (wt.%).

C	P	Si	Mn	S	Cr	Ni	Mo	Cu	Sn	Fe
0.008	0.007	0.005	0.048	0.003	0.015	0.014	0.009	0.001	0.002	Balance

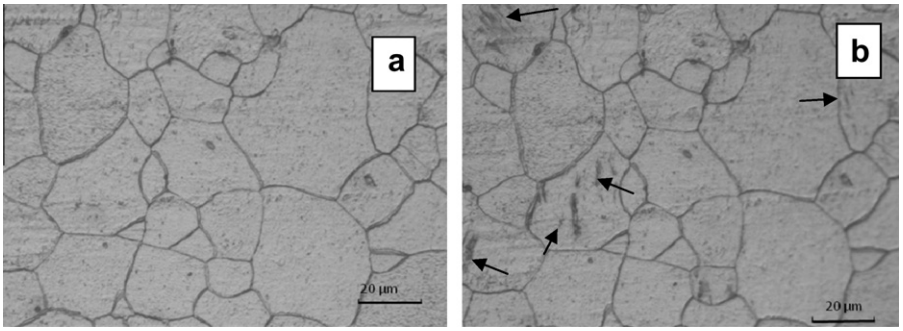

Fig. 3. (a) Before fatigue; (b) first PSB, 111 MPa after 10^8 cycles.

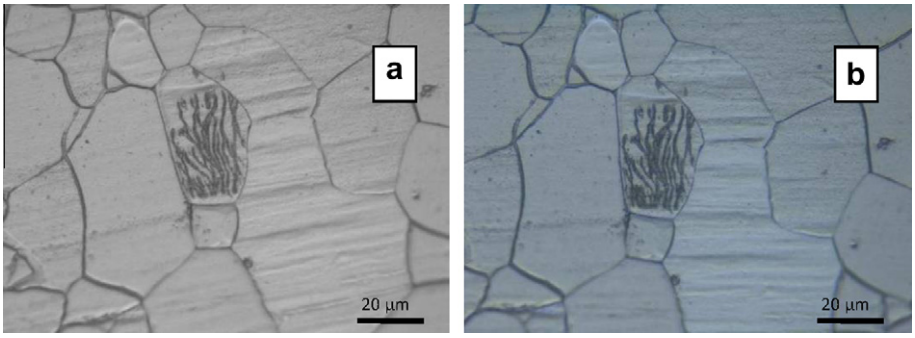

Fig. 4. Micrograph at 111 MPa (a) after 10^8 cycles; (b) after 2×10^9 cycles.

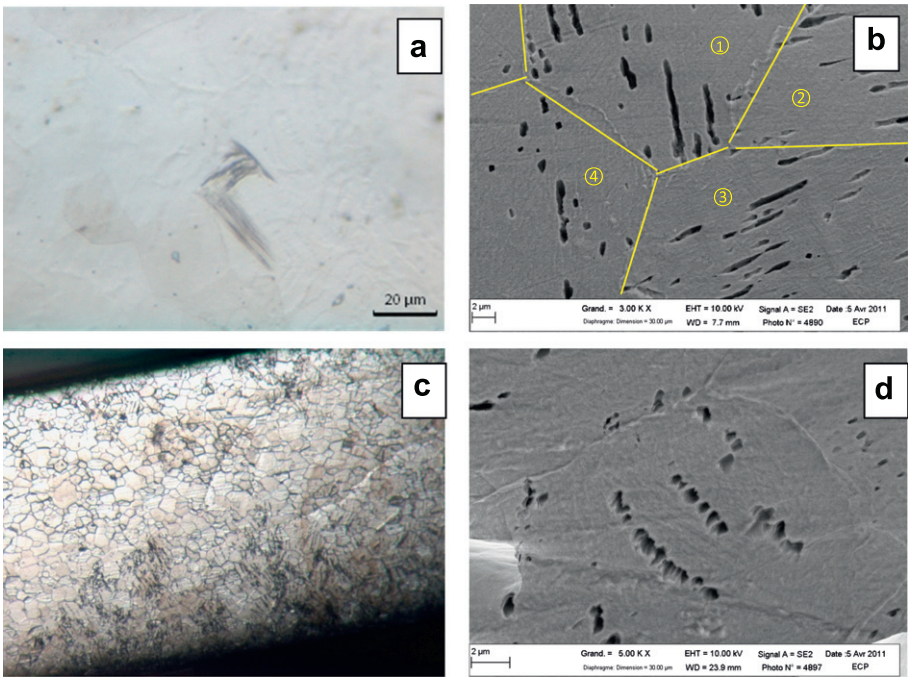

Fig. 5. (a) PSB appearances at electro polished surface; (b) PSBs at subsurface; (c) and (d) plastic deformation beneath the surface.

the specimen has free residual stress at surface. Each PSBs formed separately at different orientation with a length about 20 μm that is the same scale of grain size. Somehow PSBs stop at a sort of boundary even that grain boundary cannot be detect by optical microscopic. For another specimen which has high density of PSBs, after remove off a thin layer and etching, PSBs appeared remain inside of the grain discontinuously, Fig. 5b. Form of PSB has good agreement with the result of Klesnil et al. [10–13,22] which tested in the conventional fatigue machine at low cycle fatigue regime so called bamboo structure. This micrograph also verified that PSBs can have multi orientation in different grain and stop at grain boundary. A cross section of specimen was observed intent to investigate how deep PSBs could go through the surface. Fig. 5c shows PSBs density decrease gradually from surface to internal

and vanish after a distance of dozen grains. That deformation remains in subsurface may explain why the PSBs could reappear at same location after polishing and retest some cycles. The discontinuously points were observed in linear at this cross section at the area close to surface, Fig. 5d.

3.3. Microcrack

One specimen was tested at σ_a = 120 MPa. After 10^8 cycles scanning Electron Microscope (SEM) was used to study in higher magnification. Fig. 6a shows that PSB stopped at grain boundary. A microcrack (1 μm width and 16.4 μm long) initiated by the inharmonious of deformation at ferrite grain boundary between the grains with and without PSB. On other hand, because PSBs remain a depth inside of grain, localized irreversible deformation could also induce a microcrack, Fig. 6b. Roughness scan was taken according the path as red line in Fig. 6c. There is a significant extrusion with 1 μm high (Fig. 6d).

According to the assumption that surface roughness has developed by unknown irreversibility, a semi-quantitative approach can be used to obtain the cumulative irreversible shear strain at PSBs, which method has used on f.c.c metal. Specimen in Fig. 6c has the maximum shear stress $\tau = \sigma_a/2$ = 60 MPa in tension–compression fatigue.

Namely shear strain $\gamma_{matric} = \tau/G = 7.5 \times 10^{-4}$, where G is the shear modulus, $G = 8 \times 10^4$ for Armco iron. Approximately [23],

$$\gamma_{pl,PSB} = 15\gamma_{matric} = 10^{-2}$$

Plastic shear strain at PSBs is sufficient to nucleate a microcrack.

3.4. Fatigue crack

Fig. 7 shows an entire width of surface with fatigue failure. Crack initiated from left and propagated until a certain length then come to the final crack where has occurred a macro scale deformation. Heat diffusion appeared in front of the final crack due to the over balance between thermal transmission and cumulative thermodynamic dissipation in plastic zone of fatigue crack tip when crack propagated at this position. PSBs either were observed on surface in crack initiation area or in propagate area. However, PSBs density in initiation area is higher than the density in final crack area. Illustration of high PSBs density appears at thermodynamic dissipation area could due to the temperature increase and stress concentration occurred at crack tip.

3.5. Fractographic

Fractographic showed at Fig. 8a demonstrated the path of fatigue crack evolution. Three different areas are observed. Stage 1: initiation, stage 2: crack propagation and final stage: visible deformation. At front edge of stage 1, fatigue stress intensity factor ΔK_I = 7.6 MPa $m^{1/2}$. It corresponds to threshold of fatigue stress intensity factor ΔK_{th} of Armco iron [24], It means that the propagation at stage 1 is below the threshold corner of the Paris law. Fractographic appears either intergranular (Fig. 8b) or transgranular (Fig. 8c) at stage 1. Traces of PSBs are observed in the both models of fractographic. When crack was propagateing at stage 2, fatigue striations occurred with the same vein as transgranular crack at stage 1, Fig. 8d. But it can be distinguished because the veins of striation uniquely perpendicular to the path of crack propagation.

3.6. PSBs threshold

Specimen tested at low amplitude, fatigue stress σ_a = 88 MPa after 5.3×10^9 cycles (Fig. 9b), does not show any observable deformation, compared to the optic micrograph in Fig. 9a (initiation state). No localized irreversibility deformation appears on en-

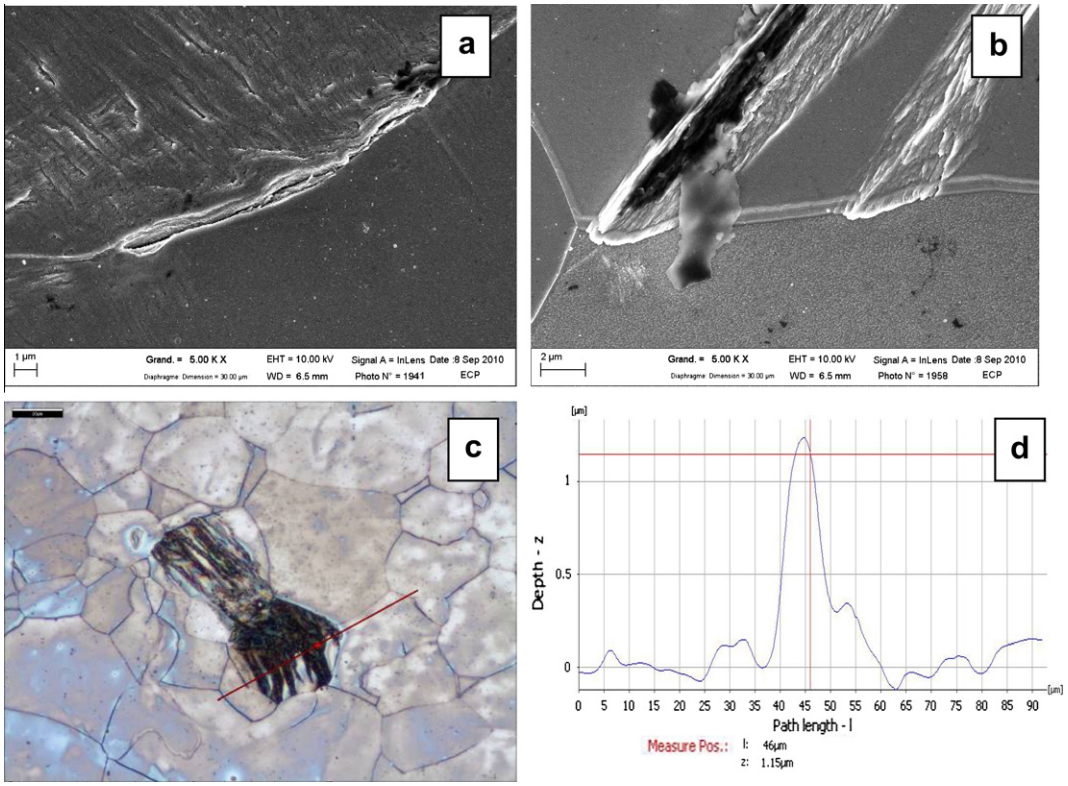

Fig. 6. (a) Microcrack along grain boundary; (b) microcrack in PSBs; (c) path of roughness scanning; and (d) roughness result.

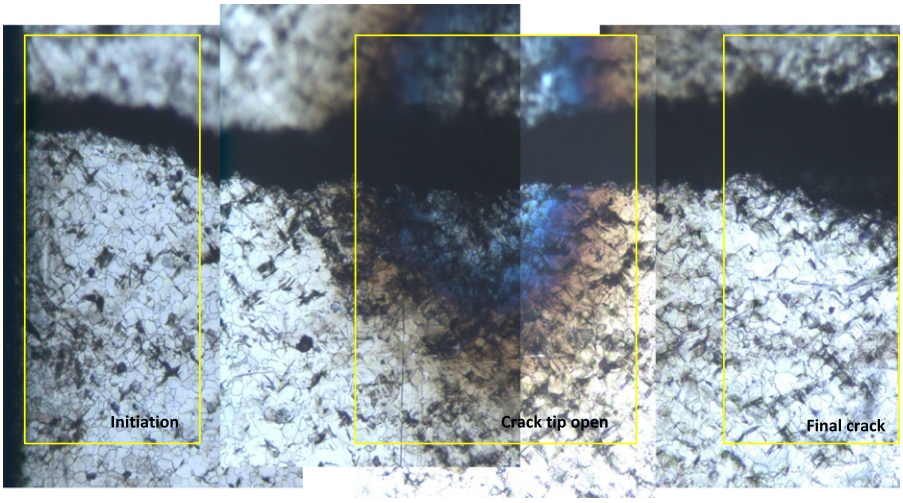

Fig. 7. Specimen surface after fatigue failure.

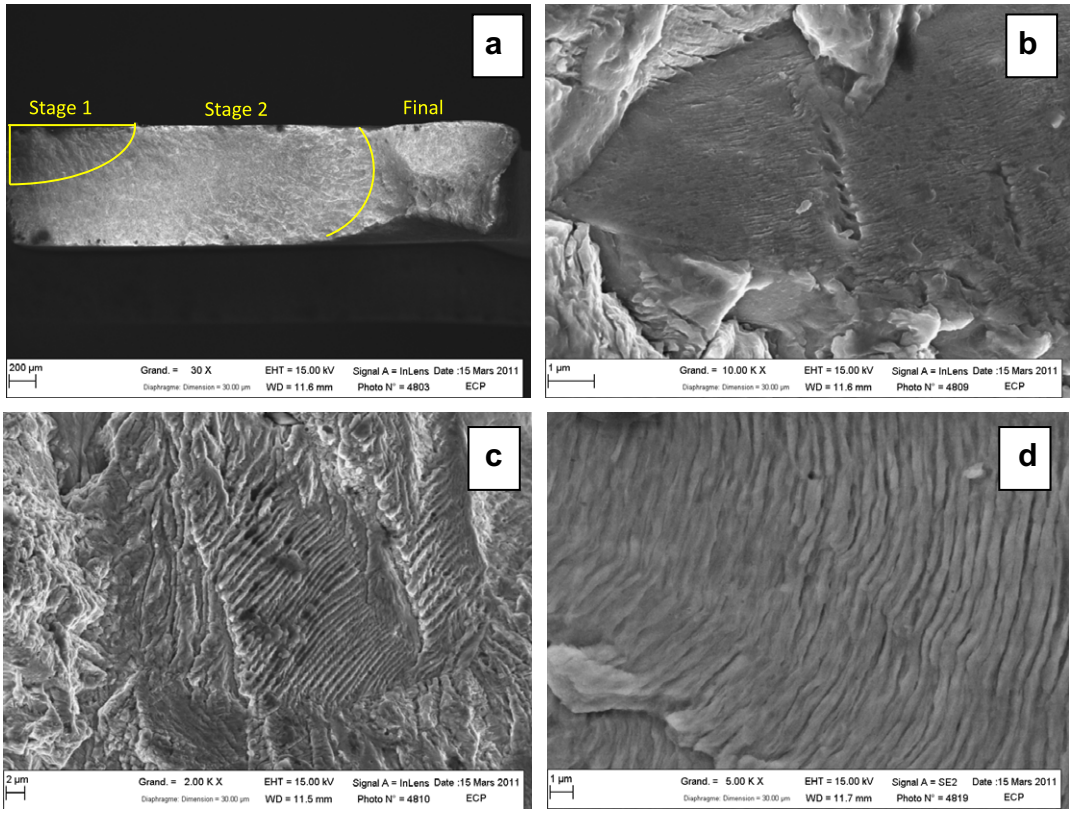

Fig. 8. (a) Fractographic; (b) intergranular crack at stage 1; (c) transgranular crack at stage 1; (d) striation at stage 2.

tire area at the low stress after very high cycle loading. However, we cannot conclude that this stress is the fatigue limit. It is only a PSB threshold for a given number of cycles.

3.7. Thermal measurements

Infrared camera was used to measure the thermal distribution on the specimen surface during fatigue tests. For the very high cycle fatigue test, the temperature rapidly increases from 290 K (ambient) and keeps almost stabilizes after 10^7 cycles due to the balance between heat resource and heat transfer, for example temperature steadies around 380 K at 120 MPa. At same loading stress (103 MPa), two specimens with different surface roughness were tested. No effect of the surface roughness was detected on the surface temperature field including microplasticity concerned (see Fig. 10). At different loading amplitude on specimen, the higher applied stress induced the larger increasing in temperature. Since temperature is important to the PSBs formation on the b.c.c crystal during fatigue loading, thermal approach should be investigated when study mechanism of crack initiation on b.c.c. metal.

Fig. 9. (a) Before fatigue; (b) micrograph after 5.3×10^9 cycles at 88 MPa.

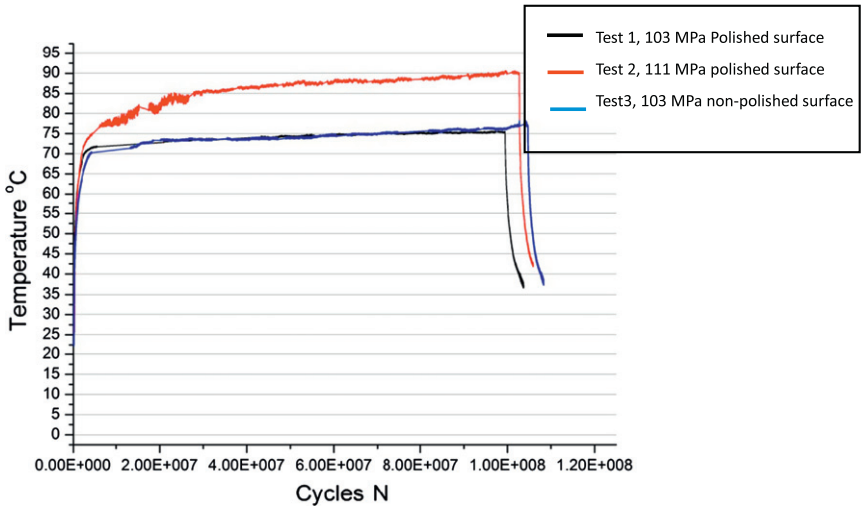

Fig. 10. Thermal measurements during interrupted tests with infrared camera.

4. Conclusion

It is found that Armco iron can failed up to 10^9 cycles in spite of the very small size of inclusions which are not operating as initiation location. For this single phase low alloy, the initiation mechanism is always related to slip bands called PSB. There is no basic difference in the PSB versus the number of cycles to failure. All the PSBs occur at the surface of the specimen even at 10^9 cycles.- Roughly speaking it seems that the density of PSB at initiation decreases in gigacycle fatigue. In flat specimen, a transition between initiation and propagation appears corresponding to the stress intensity threshold.

In the gigacycle fatigue regime, there is a competition between PSBs and grain boundary cracking in Armco iron depending of the temperature. The transition temperature should be around 50 °C.

Acknowledgements

This research was supported by the grant from the project of Microplasticity and energy dissipation in very high cycle fatigue (DISFAT, Project No. ANR-09-BLAN-0025-09), which funded by the National Agency of Research, France (ANR). The authors thank Andre Pineau and Steve Antolovich for their discussions.

References

[1] Bathias Claude. Influence of the metallurgical instability on the gigacycle fatigue regimen. Int J Fatigue 2010;32(3):535–40.
[2] Wagner D, Ranc N, Bathias C, Paris PC. Fatigue crack initiation detection by an infrared thermography method. Fatigue Fract Eng Mater Struct 2010;33(1):12–21.
[3] Chan Kwai S. Roles of microstructure in fatigue crack initiation. Int J Fatigue 2010;32(9):1428–47.
[4] Mughrabi Hael. Specific features and mechanisms of fatigue in the ultrahigh-cycle regime. Int J Fatigue 2006;28(11):1501–8.
[5] Wood WA, Mason WP. Fatigue mechanism in iron at ultrasonic frequency. J Appl Phys 1969;40(11):4514–6.
[6] Puskar A. Crack and slip band formation in iron during ultrasonic fatigue at various temperatures. Eng Fract Mech 1978;10:187–95.
[7] Mcgrath JT, Bratina WJ. Dislocation structures in fatigued iron–carbon alloys. Philos Mag 1965;12:1293–305.
[8] Wood WA, Reimann WH, Sargant KR. Comparison of fatigue mechanisms in bcc iron and fcc metals. Trans Metall Soc AIM 1964;230:511–8.

[9] Wei RP, Baker AJ. Observation of dislocation loop arrays in fatigued polycrystalline pure iron. Phil Mag 1965;12:1087–91.
[10] Klesnil M, Lukáš P. Dislocation arrangement in the surface layer of α-iron grains during cyclic loading. J Iron Steel Inst 1965(October):1043–7.
[11] Mughrabi H, Ackermann F, Herz K. Persistent slip bands in fatigued face-centered and body-centered cubic metals. Fatigue Mech ASTM-STP 1979;675:67–105.
[12] sommer C, Mughrabi H, Lochner D. Influence of temperature and carbon content on the cyclic deformation and fatigue behavior of α-iron. Part I: Cyclic deformation and stress-behavior. Acta mater 1998;46(5):1527–36.
[13] sommer C, Mughrabi H, Lochner D. Influence of temperature and carbon content on the cyclic deformation and fatigue behavior of α-iron part II: cyclic deformation and stress-behavior. Acta mater 1998;46(5):1537–46.
[14] Mughrabi H, Herz K, Stark X. Cyclic deformation and fatigue behavior of α-iron mono- and polycrystals. Int J Fract 1981;17(2):198–218.
[15] mughrabi H, Herz K, Stark X. The effect of strain-rate on the cyclic deformation properties of α-iron single crystals. Acta Metall 1976;24:659–68.
[16] Mughrabi H, Wuthrich CH. Asymmetry of slip and shape changes during cyclic deformation of α-iron single crystals. Phil Mag 1976;33(6):963–84.
[17] Poláka J, Vašek A. Fatigue damage in polycrystalline copper below the fatigue limit. Int J Fatigue 1994;16(6):403–8.
[18] Hu YM, Wang ZG. Grain boundary effects on the fatigue deformation and cracking behavior of copper bicrystals. Int J Fatigue 1998;20(6):63–469.
[19] Weidner Anja, Amberger Dorothea, Pyczak Florian, Schönbauer Bernd, Stanzl-Tschegg Stefanie, Mughrabi Hael. Fatigue damage in copper polycrystals subjected to ultrahigh-cycle fatigue below the PSB threshold. Int J Fatigue 2010;32(6):872–8.
[20] Li P, Zhang ZF, Li SX, Wang ZG. Comparison of dislocation patterns in cyclically deformed fcc metals. Scripta Mater 2008;59:730–3.
[21] Melisova D, Weiss B, Stickler R. Nucleation of persistent slip bands in Cu single crystals under stress controlled cycing. Scripta Mater 1997;36(9):1061–6.
[22] Chu RQ, Cai Z, Li SX, Wang ZG. Fatigue crack initiation and propagation in an α-iron polycrystal. Mater Sci Eng, A 2001;313:64–8.
[23] Mughrabi H. Microscopic mechanisms of metal fatigue strength of metals and alloys. In: Proceedings of the fifth international conference, Aachen, West Germany, Canada, 27–31 August 1979; 1980. p. 1615–38.
[24] Pokluda J. Characterization of crack tip stress fields. (UD) Italy: Forni di Sopra; March 7–9 2011. p. 162–9.